JOURNAL INDIAN ASSOCIATION OF SEDIMENTOLOGISTS ISSN NO 2582 – 2020
Vol. 40, Issue II, 2023, pp. 3-13
DOI: https://doi.org/10.51710/jias.v40iII.304

Provenance and Diagenetic Features of Sandstones in the Surma -Tipam Transitional Sequence exposed in the Schuppen Belt, Naga Hills, NE India

Borgohain, P.* and Pandey, N.
Department of Earth Sciences, Assam University, Silchar, Silchar-788011, Assam, India
E-mail Address: pranamee14@gmail.com

ABSTRACT
The Schuppen Belt, a part of the Indo-Burma Ranges is basically comprised of molasses of Tertiary age. This tectono–stratigraphic belt is restricted by two major thrust faults, namely Disang and Naga. In the southern part of the Naga Hills a significant part is occupied by Surma–Tipam Transitional Sequences (STTS). This study deals with the petrography, provenance, and tectonic setting of the STTS sandstones. The sandstones are classified as arkose and arkosic wacke types. The major contribution of detritus has been observed from the recycled orogen, dissected arc, transitional continental and basement uplift. The geochemistry data reveals that the sandstones were derived from a collisional setting of an active continental margin. The low degree of chemical maturity indicates that the sandstones were deposited in an arid climatic condition. The diagenetic signatures observed in these sandstones such as, point, long and concavo-convex grain boundary, albitization, crushing and squashing of quartz grains, warping of mica around detrital grains, and bending of mica suggest early to a late stage deep burial diagenesis.

KEYWORDS: **Petrography, Provenance, Diagenesis, Tectonic setting, Surma-Tipam Transitional Sequences, Naga-Hills**

INTRODUCTION

Naga Hills, the northern extension of Indo – Burma Wedge occupies a significant part of the Assam-Arakan Basin. Stratigraphically it consists of Tertiary sediments, Cretaceous Ophiolites, Precambrian metasediments and limestone clasts (Table 1). The region is divided into three morphotectonic belts having NE – SW trend, from east to west namely: Schuppen Belt, Inner Fold Belt, and Ophiolite Belt (Ghose et al. 1987). The Schuppen Belt is characterized by sediments ranging from Oligocene to Recent in age (Evans, 1964). The belt consists a narrow lineament of multiple thrust slices. Besides its two bounding thrusts i.e. Naga Thrust and Disang Thrust two other prominent thrusts of the belt are Chumliyanchen and Pephima. The Inner Fold Belt, bounded by Disang Thrust and Ophiolite Belt is characterized by Disang – Barail Transitional Sequence and Disang Group. This study is focused on the Neogene Surma – Tipam Transitional Sequences (STTS) exposed in the southwestern part of the Schuppen belt in the Dimapur District. The Surma – Tipam Transitional Sequence of the study area possess a heterogeneous lithology resembling both Surma and Tipam group of rocks (Borgohain & Pandey, 2016). The argillaceous lithology of

TABLE 1:Tertiary succession of Nagaland (Modified after Mathur and Evans, 1964; DGM, 1978; Ghose et al., 2010).

Age	Group	Lithology		
		Outer and Intermediate Hills		Eastern High Hills
Recent - Pleistocene		Alluvium and high-level terraces		
	Dihing	Boulder beds		
--------Unconformity--------				
Mio-Pliocene	Dupitila	Namsang Beds		
--------Unconformity--------				
Miocene	Tipam	Girujan Clay Tipam Sandstone		
	Surma	UpperBhuban/(STTS?) LowerBhuban		
--------Unconformity--------				
Oligocene	Barail	Renji	Tikak Parbat	Jopi / Phokphur FormationTuffaceous shale, sandstone, greywacke,grit and conglomerate. Minor limestoneand carbonaceous matter
		Jenam	Baragolai	
		Laisong	Naogaon	
UpperCretaceous-Eocene	Disang	Upper		Shale/slate/phyllite with calcareous lenses in basal sections
		Lower		Metamorphosed sediments with phyllite
--------Fault/Thrust--------				

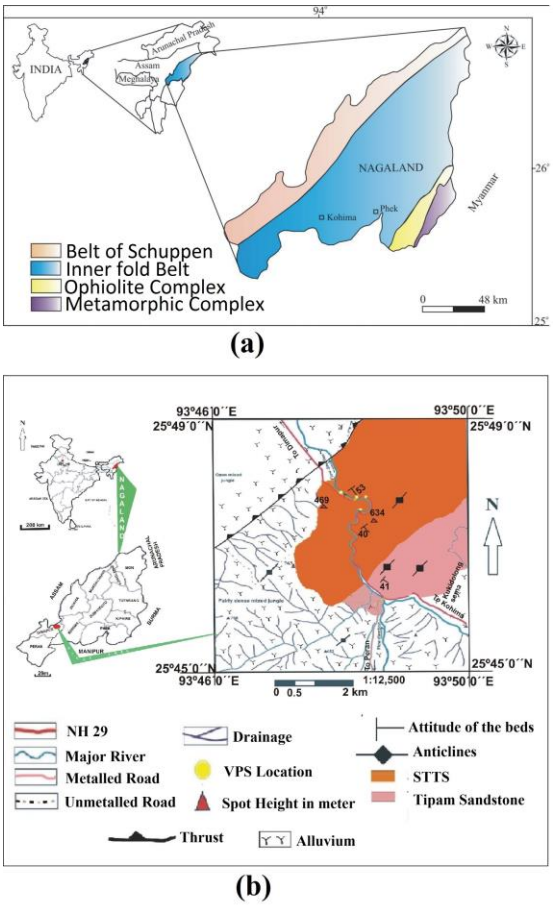

Fig (1a). Morphotectonic belts of Naga Hills after Ghose et al. (1987) **(b).** Geological map of the Study Area showing sample locations

The aim of this study is to infer the provenance, tectonic setting and diagenetic signatures of sandstones in the Surma – Tipam transitional sequences. This study investigated the maturity, provenance, transport processes and diagenetic history of sandstones. Composition of sandstones helps in deciphering the nature of petrographic province and tectonic regime that prevailed during sedimentation (Tawfik et al., 2018). It also explains the denudation history of sediments besides changes that occurred during its deposition. The present investigation is expected to help the ongoing research activities focusing on provenance studies.

STUDY AREA

The study area forms a part of the Belt of Schuppen that lies in the western margin of Nagaland (Fig 1 a). Besides well developed Surma – Tipam Transitional Sequences (Fig. 2), Tipam Sandstone Formation of the Tipam Group of Rocks and Namsang Beds of the Dupitila Group are the major lithological units observed in the study area. The Naga thrust is the major structural feature that passes through the area.

The area is bounded by the latitudes 25°45′00′′N - 25°49′00′′N and longitudes 93°46′00′′E - 93°50′00′′E of the topographic sheet no. 83G/13 of the Survey of India (Fig. 1 b). It covers almost five km distance along the NH 29 from Chumukedima town towards Kohima in Dimapur District.

sequence becomes rich in arenaceous content incorporated to the younger arenaceous Tipam Sandstone Formation. The sequence offers a local gradational passage between Surma and Tipam group of rocks instead of representing a typical Bhuban Formation in the study area.

The chemical composition of clastic sediments is a key to understand the provenance, tectonic setting, maturity, and weathering of the source region (Armstrong-Altrin et al., 2013; Basu, 2020). Numerous studies addressed the provenance of clastic sediments based on geochemistry data (Ramos-Vázquez et al., 2017; Armstrong-Altrin et al., 2021, 2022; Madhavaraju et al., 2021; Singh et al., 2023).

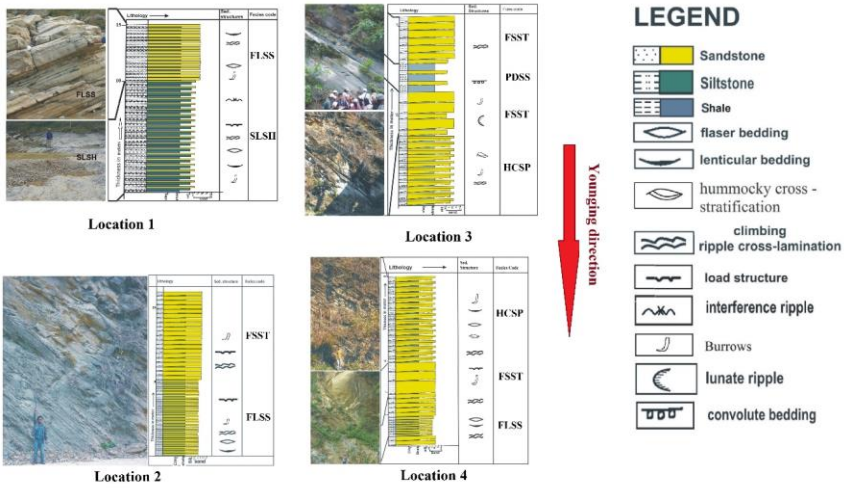

Fig 2: Vertical Profile section showing STT Ssandstones

MATERIALS AND METHODS

Twenty-four thin sections of representative sandstone samples from the

TABLE 2**:** Modal composition of STTS sandstones; (Qmt: Monocrystalline quartz, Qpt: Polycrystalline quartz)

Sample No	Quartz	Qmt	Qpt	Feldspar	Mica	Rock fragment	Matrix	Cement
RP11	21.2	15.2	7	20.5	3	2.4	25.2	5
RP12	30	21.2	8.8	20.1	7.5	2.1	12.9	20.5
RP18	32.3	22.6	9.7	18.4	5.9	6.9	25	9.9
RP19	33.6	24.3	9.3	15	13.4	7.7	6.1	23.5
RP20	40.5	24.4	16.6	28.6	5.3	0.6	7.1	11
RP21	25	10.8	14.2	15.2	9.2	5.1	30.2	15.3
RP23	21.9	14	7.9	20.2	7.2	3.1	36.2	9.8
RP24	24.7	14.6	10.1	21	6	5.3	27.5	15.5
RP25	24.5	16.4	8.1	18.3	7.5	7	7.5	38
RP26	34	29.3	4.7	15	3	5	2	40
RP28	27.8	21	6.8	22	8.8	7.8	5.4	26.3
RP29	37.1	25.8	11.3	24.7	6.47	8.07	9.07	16.5
RP30	30.6	23.6	6.9	17.2	2.1	8.1	8.5	32.8
RP31	30.6	19	11.6	28.1	6.6	13.2	6.6	13.2
RP32	31.7	17.6	14.1	28.8	6.8	11.2	7.2	10.4
RP33	31	19.8	11.2	28.1	6.1	12.8	6.7	13.4
RP 34	33	19.5	13.5	26.1	8.3	10.6	6.1	14
RP35	34.7	18	16.7	27.3	7.2	11.7	8.3	10.8
RP36	31.9	19.7	11.3	28.5	8.2	11.4	7.9	12.1
RP37	33.6	19.4	14.2	24.3	7.9	12.1	7.7	14.4
RP38	30.7	16.2	14.5	28.2	6.7	12.8	6.8	14.8
RP42	29.9	16	13.9	18.5	2.6	7.3	9.3	30.6
RP45	29	21.2	7.8	21.1	8.5	8	11.9	21.5
RP 46	30	21.7	8.3	20.4	9.1	6.2	12.1	22.2

Neogene STTS were accomplished using Leica DM LP petrological microscope in the Department of Earth Science, Assam University, Silchar. The thin sections were prepared at the department of Geological Sciences, Gauhati University. Along with thin-section study modal analysis were also carried out. More than 400 grains were counted in each thin section following Gazzi-Dickinson method (Table 2). The data on modal composition were recalculated to 100% and the sandstones were classified by following the scheme suggested by Dott (1964) and Pettijohn et al. (1987). In this scheme quartz, feldspars and rock fragments are considered as the three poles of the triangle. The demarcation between arenite and wacke has been considered at 15% (Pettijohn et al., 1987). In addition, the QtFL (total quartz-feldspar-lithic fragments) and QmFLt (monocrystalline quartz- feldspar-lithic fragments + polycrystalline quartz) diagrams of Dickinson et al. (1983) were used to discriminate tectonic provenance of the Neogene sandstones.

To identify the heavy fractions in sandstones heavy mineral analysis was done by density separation technique suggested by Folk (1980) and Middleton (2003). Separation was done using the heavy liquid bromoform.

X-ray fluorescence (XRF) spectrometry was employed to determine the major element compositions of the sandstones. Approximately 25 gm of each powdered siliciclastic rock samples was analyzed using PANalytical AXIOS Sequential X-ray Fluorescence Spectrometer and Bruker S4 Poinner Spectrometer at Sophisticated Analytical Instrument Facility (SAIF), Gauhati University and IIT Roorkee, respectively.

RESULTS AND DISCUSSION

PETROGRAPHY

The framework grains of STTS are mainly composed of quartz, feldspars and rock fragments. Other minerals include muscovite, biotite, chlorite, glauconite and heavy minerals. The cementing materials are dominated by silica, iron - oxide and calcite (Table 2).

According to the classification scheme of Pettijohn et al. (1987), these sandstones dominantly represents arkose and arkosic wacke types (Fig. 3). Among the framework grains quartz is the most dominant variety. It includes monocrystalline undulatory non – undulatory, polycrystalline quartz grains.

Feldspars are the second most dominating framework grains of STTS sandstones. Among feldspars, plagioclase dominates over k-feldspar. K-feldspars include orthoclase, microcline and sanidine. Orthoclase dominates over the others. Feldspars grains possess sub-rounded to angular outlines. Rock fragments are composed of all three varieties, i.e. sedimentary, metamorphic and igneous. Shale, siltstone and sandstones are the common varieties of sedimentary rock fragments. While physillite and volcanic rock fragment characterize the metamorphic and igneous varieties, respectively.

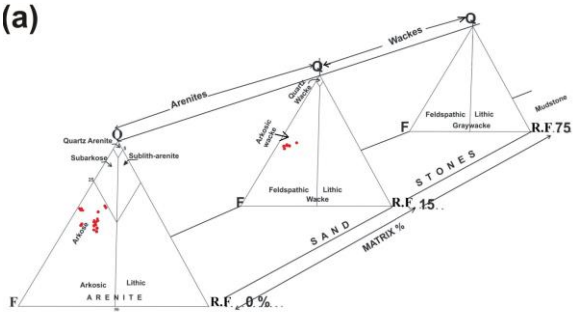

Fig 3: Classification of STTS sandstones after Pettijohn et al. (1987)

Among micas muscovite and biotite are the dominating varieties. Some flakes of chlorite, glauconite and illite are also observed in fine-grained samples. Matrix is mainly composed of

sericite and chert. Different types of grain contacts such as point, long, rare concavo–convex, sutured and isolated or floating grains of STTS sandstones depicts different degrees of compaction.

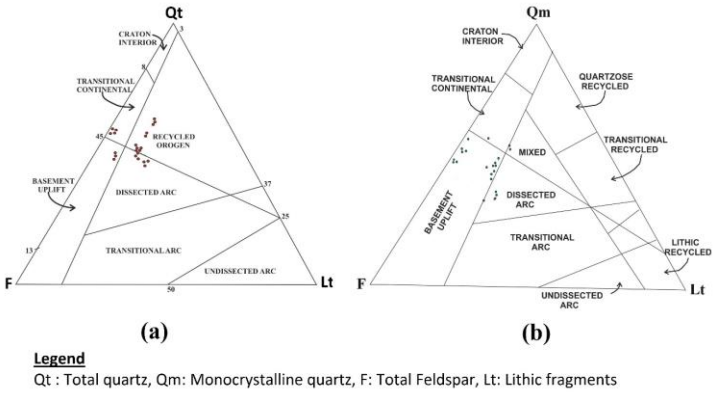

Fig 4: QtFLt and QmFLt after Dickinson and Suczek (1979) and Dickinson et al. (1983) showing the tectonic provenance of STTS sandstones.

TECTONIC PROVENANCE

Petrographic and geochemistry data have been widely used in various studies to understand the nature of the tectonic provenance of clastic sediments and rocks (Verma and Armstrong-Altrin, 2013, 2016; Verma et al., 2016; Bessa et al., 2021; Bela et al., 2023). In this study, both of the mentioned approaches have been utilized to understand the nature of the tectonic provenance of STTS sandstone. In order to interpret the tectonic setting of STTS, the triangular plots of QmFLt and QtFLt after Dickinson et al. (1983) and Dickinson and Suczek (1979) were used. On these diagrams the sandstones show a mixed contribution of dissected arc, basement uplift, transitional continental and recycle orogen, indicating an active tectonic setting in the source area (Fig 4).

HEAVY MINERALS

The nature of heavy mineral suites of STTS sandstones reflects intermingling of various provenance of the sedimentary sequence. The heavy mineral suite constitutes opaque and non – opaque varieties. Non – opaque varieties dominate over the opaque varieties. The percentage of opaque and non – opaque heavy minerals is graphically represented in Fig. 5 a. The opaque grains assumed to be iron oxide. The non–opaque transparent varieties include tourmaline, rutile, zircon, kyanite, sillimanite, sphene, dolomite, hornblende, phlogopite, clinohumite, humite, chondrodite, scapolite, staurolite, cordierite, garnet, xenotime, vesuvianite, epidote, zoisite, clinozoisite, hedenbergite, apatite and chloritoid (Fig. 6). Among the non – opaque varieties zircon, tourmaline, rutile, garnet, staurolite, chondrodite, humite and epidote dominate over the others. Most of the zircon grains possess subhedral to rounded shape. Twinned staurolite and epidote grains are not common. Among the tourmaline varieties schorlite dominates over dravite. Anatase and brookite two varieties of rutile are also observed in studied STTS sandstones. Though most of the garnets are subhedral to rounded in shape, some fine-grained euhedral grains are also observed.

MINERALOGICAL MATURITY

The mineralogical maturity of sandstone can be depicted on the basis of the presence of stable and unstable

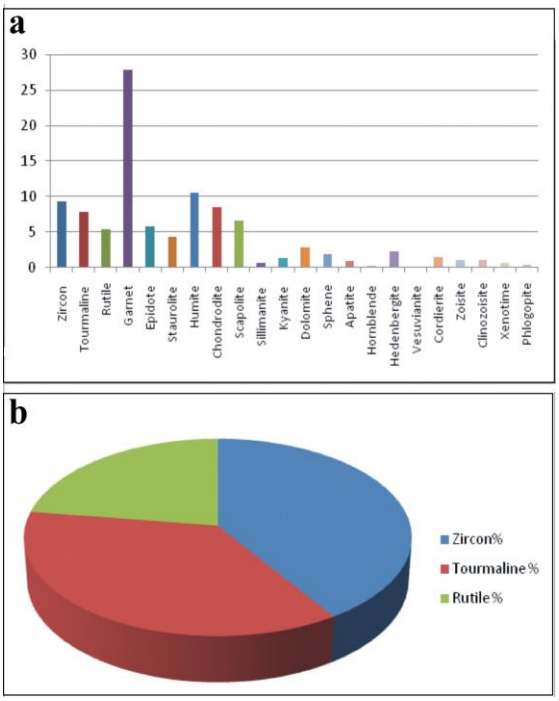

Fig 5 a: Graphical representation of heavy minerals distribution in the STTS sandstones **(b):** Graphical representation zircon tourmaline and rutile distributions in the STTS sandstones

constituents, i.e. increasing percentage of stable constituents such as quartz, chert etc. indicates higher degree mineralogical maturity and increasing percentage of unstable constituents such

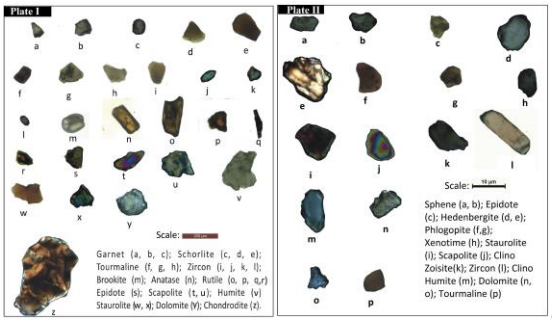

Fig 6: Different heavy minerals observed in STTS sandstones

s feldspars and rock fragments, suggesting lower degree of mineralogical maturity (Folk 1980). Besides these ZTR index of heavy minerals is also a good indicator of mineralogical maturity. The average ZTR index of STTS is found to be 20.9 % depicting mineralogically an immature nature. The presence of higher percentage of feldspar and rock fragments of sandstone further supports the immature to sub-mature nature of the sandstones.

TABLE 3:Major element concentrations of STTS sandstones (in wt. %)

S No	SiO_2	Al_2O_3	Fe_2O_3	MnO	MgO	CaO	Na_2O	K_2O	TiO_2	P_2O_5	Total
P4	68.61	13.7	4.91	0.04	3.240	2.15	1.71	2.94	0.60	0.14	98.04
P5	49.45	6.28	3.10	0.10	2.605	14.3	1.48	1.49	0.56	0.16	79.525
P6	38.08	6.79	5.17	0.15	2.689	20.1	1.21	2.20	0.39	0.23	77.009
P7	64.55	9.72	4.26	0.03	3.540	1.72	1.75	2.09	0.56	0.15	88.37
P8	65.16	9.99	4.61	0.04	3.849	2.01	1.74	2.10	0.58	0.16	90.239
P9	51.29	9.28	7.22	0.05	4.156	2.47	1.44	1.61	0.69	0.15	78.356
P10	64.63	10.2	4.27	0.04	1.978	0.93	1.75	2.24	0.52	0.15	86.708
P14	72.49	8.48	5.86	0.08	0.50	2.76	2.20	2.30	0.70	0.14	93.21
P15	72.40	13.01	4.45	0.07	0.60	1.84	2.17	2.13	0.45	0.16	97.28

PROVENANCE

Heavy mineral constituents can lead us to understand the nature of the tectonic provenance of sandstones. On the basis of occurrences of heavy minerals in STTS, the following four assemblages are identified along with their source rock characteristics.

(i) Humite – Clinohumite – Chondrodite – Phlogopite – Scapolite – Wollastonite – Sphene – Tourmaline (Dravite) – Vesuvianite – Epidote – Brookite – Iron oxide, which characterizes a contact dolomitic marble and scarn source rocks.

(ii) Zircon – Tourmaline (Schorlite) – Sphene – Apatite – Hornblende – Hedenbergite is an indicative of granite and granitoid sources.

(iii) Tourmaline (Schorlite) – Kyanite – Sillimanite – Staurolite – Hornblende – Hedenbergite – Rutile – Anatase – Garnet signifying a regionally metamorphosed source terrain.

(iv) Tourmaline (Scorlite and Dravite) – Garnet – Xenotime indicates pegmatitic source.

(v) Rounded reworked grains of Zircon – Tourmaline – Rutile – Dolomite etc. indicate a sedimentary source terrain.

MAJOR ELEMENT CONCENTRATIONS

A total of ten representing sandstone samples were analyzed for major element concentrations (Table 3). The SiO_2 concentration of the sandstones varies between 38 and 68 wt. %, with an average of 58 wt. %. The SiO_2/Al_2O_3 ratio of STTS sandstone is relatively high. The lower level of chemical maturity of the sediments is reflected by the binary plot of $Al_2O_3+K_2O+Na_2O$ against SiO_2 (Suttner and Dutta, 1986). The major elements can provide information about the climatic condition that prevailed during the deposition of sediments. The bivariate plot of $Al_2O_3+K_2O+Na_2O$ against SiO_2 suggest an arid climatic condition for the STTS sandstones (Fig. 7 a). Source rock composition has a significant contribution to the chemical attributes of clastic rocks. Besides this, secondary processes like chemical weathering and diagenesis of clastic rocks like sandstone; shale etc. also have an effect on the chemical composition. It is also influenced by the nature of sedimentary processes that prevail in the depositional basin and the nature of transporting processes that occur from the source region to the depositional basin (Dickinson and Suczek, 1979). The geochemical composition of clastic rocks is a function of provenance, weathering, transportation and diagenesis (Mustafa, R. K., and Tobia, 2020). Condie et al. (1992) attempted to decipher the provenance characteristics using geochemical attributes of sandstones. The tectonic environment and type of provenance also can be interpreted from the major element geochemistry of a clastic sediments (Armstrong-Altrin 2015; Migani et al. 2015; Odoma et al. 2015; Zaid 2016, Kafy and Tobia, 2022). Accordingly, bivariate plot of Na_2O against K_2O after Crook (1974) suggests the derivation of STTS sandstones from a quartz rich

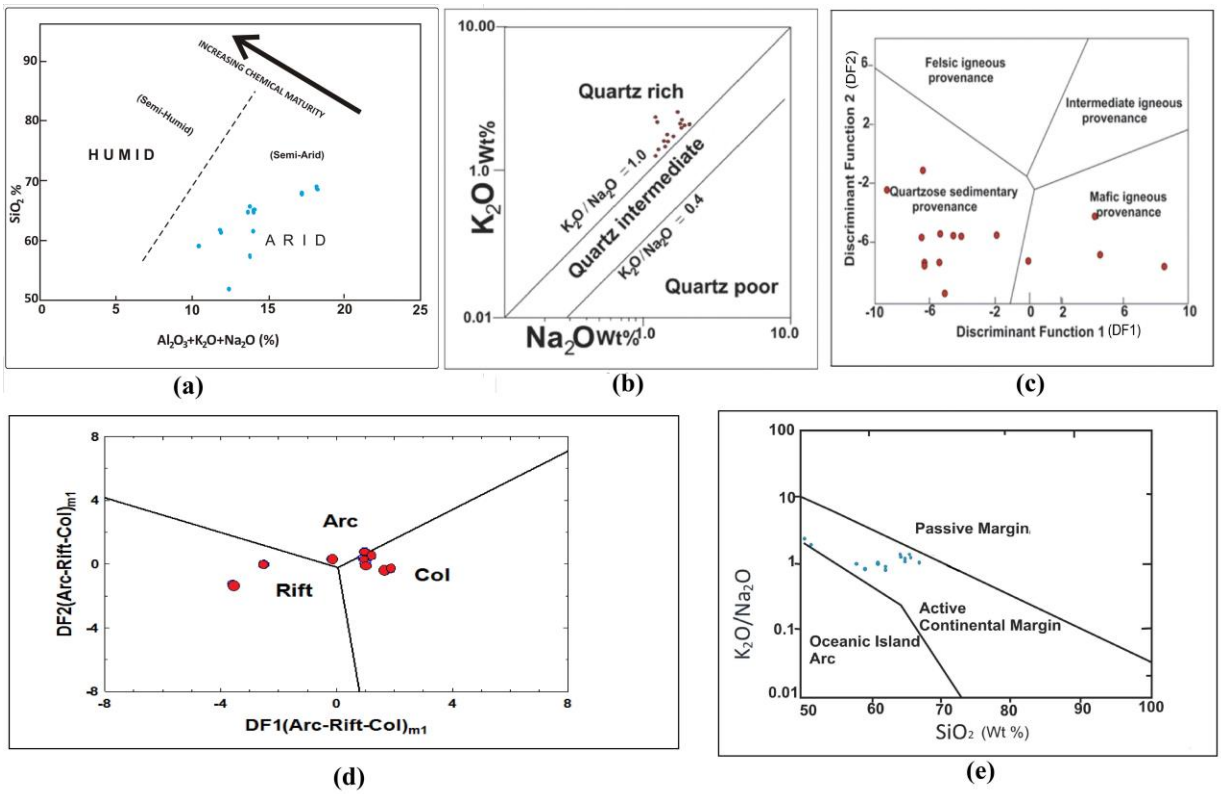

Fig 7(a): The bivariate plot of $Al_2O_3+K_2O+Na_2O$ against SiO_2 (Suttner and Dutta, 1986) suggesting an arid climatic condition forthe STTS sandstones, **(b):** Bivariate plot of Na_2O against K_2O after Crook (1974) suggests derivation of sediments from a quartz rich source, **(c):** Bivariate plot after Roser and Korsch (1988), **(d):** High-silica multidimensional diagram for the classification of tectonic settings (after Verma and Armstrong-Altrin, 2013), **(e):** Bivariate plot of K_2O/Na_2O vs. SiO_2 (Roser and Korsch, 1986) suggests an active continental margin setting for the STTS sandstones.

source (Fig. 7 b). In order to discriminate provenance, Roser and Korsch (1988) diagram has been used (Fig. 7 c). This diagram was constructed based on two discriminant functions namely DF1 and DF2, where DF1 = (– 1.773*TiO_2) + (0.607*Al_2O_3) + (0.760*Fe_2O_3) + (– 1.500*MgO) + (0.616*CaO) + (0.509*Na_2O) + (– 1.224*K_2O) + (– 9.090) and DF2 = (0.445*TiO_2) + (0.070*Al_2O_3) + (– 0.250*Fe_2O_3) + (– 1.142*MgO) + (0.438*CaO) + (1.475*Na_2O) + (1.426*K_2O) + (– 6.861). This diagram reveals mostly a quartzose sedimentary provenance for the studied sandstones.

The major elements geochemistry of sandstones can elucidate the tectonic setting of a sedimentary basin (Crook, 1974; Middleton, 1960). Siever (1979) and Roser and Korsch (1986) successfully related the proportion of detrital components to the bulk chemical composition of sedimentary suites that in turn reflect the tectonic setting of the basin. Bhatia (1983) developed a bivariate plot of Fe2O3+MgO versus K2O/Na2O wt. % to decipher the tectonic provenance of sandstones. Winchester and Max (1989) used the major elements as a geochemical tectonic indicator of immature sediments. However, in the present study, tectonic discrimination diagrams of Verma and Armstrong (2013) and Roser and Korsch (1986) are preferred to understand the tectonic provenance of the STTS sandstones. Since the adjusted concentrations of SiO_2 is higher than 62 wt.%, the high silica diagram of Verma and Armstrong (2013) is applied.

The multidimensional plot for high-silica $\{(SiO_2)_{adj}$ = > 63% - ≤ 95%} clastic sediments of Verma and Armstrong(2013) involves two discriminant functions, i.e., DF1 and DF2, where DF1(Arc–Rift–Col) m1 = (-0.263 x $In(TiO_2/SiO_2)_{adj}$)+ (0.604 x $In(Al_2O_3/SiO_2)_{adj}$) + (-1.725 x $In(Fe_2O_3{}^t/SiO_2)_{adj}$)+ (0.660 x $In(MnO/SiO_2)_{adj}$)+ (2.191 x $In(MgO/SiO_2)_{adj}$)

+(0.144 x $In(CaO/SiO_2)_{adj}$)+ (-1.304 x $In(Na_2O/SiO_2)_{adj}$) + (0.054 x $In(K_2O/SiO_2)_{adj}$)+ (-0.330 x $In(P_2O_5/SiO_2)_{adj}$) + 1.588 and DF2 $_{(Arc\text{-}Rift\text{-}Col)m1}$=(-1.196 x $In(TiO_2/SiO_2)_{adj}$)+ (1.064 x $In(Al_2O_3/SiO_2)_{adj}$) + 0.303 x $In(Fe_2O_3{}^{t}/SiO_2)_{adj}$)+ (0.436 x $In(MnO/SiO_2)_{adj}$)+ (0.838 x $In(MgO/SiO_2)_{adj}$) +(-0.407 x $In(CaO/SiO_2)_{adj}$)+ (1.021 x $In(Na_2O/SiO_2)_{adj}$) + (-1.706 x $In(K_2O/SiO_2)_{adj}$)+ (-0.126 x $In(P_2O_5/SiO_2)_{adj}$) – 1.068. The diagram reveals a collisional tectonic setting for the STTS sandstones (Fig. 7d). On the other hand, the K2O/Na2O vs. SiO2 plot of Roser and Korsch (1986) suggested an active continental margin for the sandstones (Fig. 7 e).

DIAGENESIS

A series of diagenetic signatures involving mineralogical and textural attributes are observed in STTS sequence of the study area. These diagenetic signatures are grouped into early, intermediate and late stages (deep burial diagenesis and incipient metamorphism after Borak and Friedman, 1981). Precipitation and deposition of cement (silica, calcium carbonate and iron) is one of the processes of early diagenetic changes (Fig. 8 a). Replacement of silica cement (quartz overgrowth) by the carbonate cement was followed by iron - oxide precipitation depicting a typical order of cementation (Burley et al., 1985). The sedimentary sequences of the study area possess an eogenetic assemblage of authigenic carbonate, chlorite, glauconite, feldspar and quartz (Fig. 8 b and 8c). These authigenic growths are commonly seen on quartz and feldspars (Fig. 8 c). Sporadic occurrence of 'quartz islands' depict near complete replacement of quartz by matrix (Fig. 8 d). Presence of pseudo - matrix signifies post depositional degradation of feldspars (Fig. 8 d). On the other hand, presence of euhedral feldspars points either towards authigenic growth during deep burial phase or volcanic derivation (Fig. 8 d).

Process of albitization is a common diagenetic phenomenon observed in STTS sandstones. It occurs along the plane of weakness through hydrous reaction in which An-rich plagioclase is albitized first and followed by An-poor plagioclase (Ramseyer et al., 1992). Untwinned or slightly twinned cloudy feldspars (Fig. 8 d) in STTS sandstones bear small bleb like features that extinct differently than the grain. Such feldspar grains have been attributed to albitization process (Pittman, 1988). In addition, plagioclase grains showing discontinuous twin lamellae related to partial dissolution followed by authigenic albite infilling (Gold, 1987) resembling perthite texture. Presence of unaltered fresh plagioclase and albitized plagioclase in STTS is an indicator of albitization process. Nucleation of authigenic feldspar crystals on the surface of detrital feldspars and the recrystallization of detrital plagioclase feldspars could be the reason for albitization (Michalik, 1998). Dissolution and

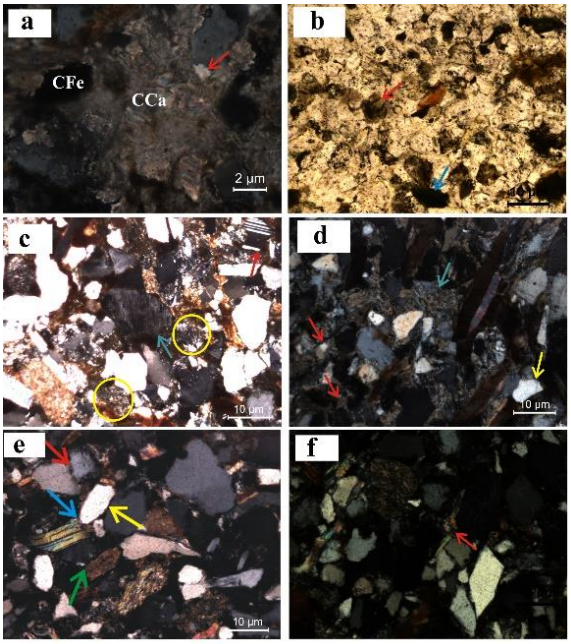

Fig 8 (a): Thin-section photograph showing typical order of cementation i.e. replacement of silica cement (red arrow) by the carbonate cement (CCa) which was followed by iron - oxide precipitation (CFe), (b): Thin-section photograph showing authigenic growth of glauconite (red arrow) and chlorite (blue arrow) as cement types, (c): Thin-section photograph showing growth of neo-quartz (yellow circle marked), authigenic growth of albite (red arrow), perthitic texture due to albitization (blue arrow), (d): Thin-section photograph showing formation of quartz by thenear complete replacement of detrital quartz by matrix (red arrow), pseudomatrix (blue arrow), fracture in quartz (yellow arrow), (e): Thin-section photograph showing different grain contacts: sutured contact (red arrow), concavo-convex contact (blue arrow), long contact (yellow arrow) and point contact (green arrow), (f): Kink bending and warping of mica around the detrital quartz grain

replacement of feldspars are the processes of formation of authigenic chlorite and glauconite which observed in some of the samples belonging to the lower part of the stratigraphic sequence. The authigenesis of chlorite could be the source of Fe cement.

Presence of calcareous cement and carbonate rock fragments in STTS sandstones indicates a depositional setting above the Carbonate Compensation Depth (CCD).

Devitrification of the volcanic glasses is considered to be one of the sources of authigenic quartz. Different phases of dissolution may have provided pore-waters with necessary components, which were essential for the authigenic growth of silica and carbonate phases (Merino, 1975 and Surdam & Boles, 1979). In the initial stage of burial, the diagenesis of detrital grains results changes in pore-water chemistry and the reaction of amorphous material and less stable detritus (Curtis, 1978).

The grain-to-grain boundaries of STTS sandstones (Fig. 8 e) show different stages of diagenesis. The concavo-convex and sutured grain-to-grain boundaries are the result of intermediate burial diagenesis. In the intermediate stage of diagenesis the grain-to-grain interlocks are formed by the dissolution of silica at the point of grain contact. Taylor (1950) suggested that the point contacts of grains are the result of two operating processes – (i) solid flow and solution and (ii) redeposition (interstitial transport of dissolved material). The compound grains are the result of increasing intensity of diagenesis that leads to the imposition of self-boundaries between two adjacent grains in close optical orientation (Dapples, 1979). The straight-line grain boundaries are the result of mobility of constituent chemical components. Under the continuous process of dip burial diagenetic evolution, the three-dimensional network of these straight-line boundaries results in the formation of the triple-junctions (Ahmad et al., 2006). Features like fracturing of detrital quartz (Fig. 8 d), crushing and squashing of detrital grains, wrappings of mica flakes around quartz grains (Fig. 8 f), pressure solutions effect and matrix are some indicator of increasing depth of burial (Burley et al., 1985). In addition, other signatures of deep burial diagenesis in the sediments of the study area include recrystallization / reconstitution of matrix and kink bending in mica (Fig. 8 f). Devitrification of volcanic glass leading to development of chert like microcrystalline aggregates, and alteration of volcanic glass into silica and clay minerals further indicate that the diagenetic processes possibly operated in a sealed environment (Pettijohn et al., 1987).

CONCLUSION

The STTS sandstones are very fine to medium- grained, sub- angular to angular, moderately to moderately well sorted. Dominating framework grains of these sandstones are quartz, feldspar, rock-fragments and micas. Different types of quartz that were found in STTS sandstones are polycrystalline undulatory, monocrystalline, recrystallized metamorphic and detrital quartz. The STTS sandstones are dominantly of arkose and arkosic wacke types.

The mineralogical composition of sandstones reveals that their source being a mixed provenance including plutonic basement, granitic intrusive, sedimentary and metasedimentary rocks. Further this inference is supported by the different provenance discriminating plots based on major elemental data.

Tectonic provenance discriminating diagrams (Qt-F-Lt and Qm-F-Lt) depict transitional continental, basement upliftment, dissected arc, and recycled orogen provenance. The tectonic discriminating plots using major elemental data reveals an active continental margin setting for the sandstones. A complex metamorphic basement and granitic intrusive sources, and an uplifted terrain like Mishimi Hills of Southern Himalaya and also Naga-Ophiolite Belt, Indo-Burma Range and prior to the Miocene sedimentary rocks of the region are considered as the most probable source rocks for STTS sandstones.

Diagenetic signatures observed in STTS belong to three different stages of diagenesis i.e. early, intermediate and late stages. Different types of grain boundaries suggest the early cementation and less compaction of the sandstone. The cementation process of the sandstone appears to be initiated by Fe cementation followed by silica cement and in some of the samples it is further followed by the calcite crystallization.

Precipitation and deposition of silica, epitaxial growth of mica around detrital quartz grains, near complete replacement of quartz by matrix and degradation of feldspars are some of the indications of early diagenetic changes of the STTS sandstone. Presence of euhedral authigenic albite represents albitization process that occurs during the burial diagenesis or intermediate stage of diagenesis. Kink bending of mica, warping of mica around quartz grains, crushing and squashing of detrital grains are indicative of deep burial diagenesis of sandstones.

ACKNOWLEDGEMENTS:

We are highly thankful to the University Grant Commission (UGC) for financial support to carry out this work. We are also thankful to the Department of USIC, Department of Geological Sciences, Gauhati University and Department of Geology, and IIT Roorkee for providing us the laboratory facility of XRF and thin section preparation. We are also thankful of Department of

Geology, Nagaland. We extend our heartfelt gratitude to the Editor of the Journal Indian Association of Sedimentologists, Dr. Amstrong-Altrin and the two reviewers of this manuscript, their suggestions and guidance improved the quality of our presentation.

DECLARATION OF CONFLICTING INTERESTS: The authors declare that they have no competing interests.

REFERENCES

Ahmad, A.H.M. and Bhat, G.M. (2006). Petrofacies Provenance and diagenesis of the dhosa sandstone member (Chari Formation) at Ler, Kachch sub – basin, Western India. Journal of Asian Earth Sciences, volume 27, pp. 857 – 872.

Armstrong-Altrin J. S. (2015). Evaluation of two multidimensional discrimination diagrams from beach and deep-sea sediments from the Gulf of Mexico and their application to Precambrian clastic sedimentary rocks; International Geological Review, volume 57, pp. 1444–1459.

Armstrong-Altrin, J.S., Nagarajan, R., Madhavaraju, J., Rosales-Hoz, L., Lee, Y.I., Balaram, V., Cruz-Martinez, A., Avila-Ramirez, G. (2013). Geochemistry of the Jurassic and upper Cretaceous shales from the Molango Region, Hidalgo, eastern Mexico: Implications for source-area weathering, provenance, and tectonic setting. Comptes Rendus Geoscience, volume 345 (4), pp. 185-202.

Armstrong-Altrin, J.S., Madhavaraju, J., Vega-Bautista, F., Ramos-Vázquez, M.A., Pérez-Alvarado, B.Y., Kasper-Zubillaga, J.J. and Ekoa Bessa, A.Z. (2021). Mineralogy and geochemistry of Tecolutla and Coatzacoalcos beach sediments, SW Gulf of Mexico. Applied Geochemistry. 134, 105103.

Armstrong-Altrin, J.S., Ramos-Vázquez, M.A., Madhavaraju, J., Marca-Castillo, M.E., Machain-Castillo, M.L., Márquez-Garcia, A.Z. (2022). Geochemistry of marine sediments adjacent to the Los Tuxtlas Volcanic Complex, Gulf of Mexico: Constraints on weathering and provenance. Applied Geochemistry, 141, no. 105321.

Basu, A. (2020). Chemical weathering, first cycle quartz sand, and its bearing on quartz arenite. Journal Indian Association of Sedimentologists, volume 37(2), pp. 3-14.

Bela, V.A., Bessa, A.Z.E., Armstrong-Altrin, J.S., Kamani, F.A., Nya, E.D.B., Ngueutchoua, G. (2023). Provenance of clastic sediments: A case study from Cameroon, Central Africa. Solid Earth Sciences 8(2), pp. 105-122.

Bhatia, M.R. (1983). Plate tectonics and geochemical composition of sandstones. Journal Geology, volume 91 (4), pp. 611–626.

Borak, B. and Friedman, G.M. (1981). Textures of sandstones and carbonate rocks in the world's deepest wells (in excess of 30,000ft. or 9.1km): Anduako Basin, Oklahoma. Journal of Sedimentary Geology, volume 29, pp. 133-151.

Borgohain, P. and Pandey, N. (2016). Lithofacies analysis of Surma-Tipam Transitional Sequences inparts of Naga Hills, Northeast India: A Case Study. Journal of Applied Geology and Geophysics, volume 5 (V), pp. 30 – 36.

Burley, S.D., Kantorowicz, J.D., Waugh, B. (1985). Clastic diagenesis. In: Brenchley, P.J. and Williams, B.P.J. (eds.). Sedimentology, Recent developments and Applied Aspects, Blackwell, Oxford, volume 18, pp. 189-226.

Condie, K.C., Boryta, M.D., Liu, J., Quian, X. (1992). The origin of khondalites: geochemical evidence from the Archean to Early Proterozoic granulite belt in the North China craton. Precambrian Research, volume 59, pp. 207–223.

Crook, K. A. W. (1974). Lithogenesis and geotectonics: The significance of compositional variation in flysch arenites (greywackes), In: R. H. Dott and R. H. Shavar (Eds.), Modern and ancient geosynclinals sedimentation, Soc. Econ. Palaeont. Min. Spl. Publ., volume 19, pp. 304 – 310.

Curtis, C.D. (1978). Possible links between sandstone diagenesis and depth-related geochemical reactions occurring in enclosing mudstones. Journal of Geological Society of London, volume 135, pp. 107–117.

Dapples, E.C. (1979). In: Larsen, G., Chinlinger, G.V. (Eds.), Diagenesis in Sandstones.Developments in Sedimentology 25A. Elsevier, The Netherlands, pp. 31–97.

Dickinson,W.R. and Suczek, C.A. (1979). Plate tectonics and sandstone compositions. American Association of Petroleum Geologists, volume 63, pp. 2164 – 2182.

Dickinson, W.R., Beard, L.S., Brakenridge, G.R., Erjave, J.L., Ferguson, R.C., Inman, K.F., Knepp., R.A., Lindberg, F.A., and Ryberg, P.P. (1983). Provenance of North American Phanerozoic sandstones in relation to tectonic setting. Geological Society American Bulletin, volume 94, pp. 222-235.

Dott, R.H. (1964). Wacke, Greywacke and Matrix—What Approach to Immature Sandstone Classification? Journal of Sedimentary Petrology, volume 34, pp. 625-632.

Ekoa Bessa, A. Z., Paul-Désiré, N., Fuh, G.C., Armstrong-Altrin, J.S., Betsi, T.B., 2021. Mineralogy and geochemistry of the Ossa lake Complex sediments, Southern Cameroon: Implications for paleoweathering and provenance. Arabian Journal of Geosciences 14, Article no. 322

Evans, P. (1964). The tectonic framework of Assam. Journal of Geological Society of India, volume 5, pp. 80 - 96.

Folk, R.L. (1980). Petrology of Sedimentary Rocks, Austin, TX, Hemphill Press, Second Edition, pp. 20 – 25.

Ghose, N.C., Agrawal, O.P. and Srivastava, S.C., 1987. Metamorphism of the ophiolite belt of Nagaland, NE India. Proceedings of National Seminar of Tertiary Orogeny, pp. 189-213

Gold, P.B. (1987). Textures and geochemistry of authigenic albite from Miocene sandstones, Lousiana Gulf Coast. Journal of Sedimentary Petrology, volume 57, pp. 353-362.

Kafy, R.H., Tobia, F.H. (2022). Geochemical signatures of provenance, chemical weathering, and tectonic setting in the Greater Zab River sediments, Iraqi Kurdistan Region. Arabian Journal of Geosciences, 15:1556**.**

Madhavaraju, J., Armstrong-Altrin, J.S., Pillai, R.B., Pi-Puig, T. (2021). Geochemistry of sands from the Huatabampo and Altata beaches. Gulf of California, Mexico. Geological Journal, 56, 2398-2417.

Merino, E. (1975). Diagenesis in Tertiary sandstones from Kettleman North Dome, California I. Diagenetic mineralogy. Journal of Sedimentary Petrology, volume 45, pp. 320 – 336.

Michalik, M. (1998). Diagenetic albite in Rotliegendes sandstones from the Intrasudetic Basin (Poland). Annales Societatis Ceologorwn Poloniae, volumen 68, pp. 85-93.

Middleton, G.V. (1960). Chemical composition of sandstones, Geological Society of America Bulletin, volume 71, pp. 1011-1026.

Middleton, G.V. (Ed), (2003). Encyclopedia of Sediments and Sedimentary rocks. Springer, pp. xxx–821.

Migani F., Borghesi F. and Dinelli E. (2015). Geochemical characterization of surface sediments from the northern Adriatic wetlands around the Po river delta, Part 1: Bulk composition and relation to local background; Journal of Geochemical Exploration, volume. 156, pp. 72–88.

Mustafa, R. K., and Tobia, F.H. (2020). Geochemical application in unraveling paleoweathering, provenance and environmental setting of the shale from Chia Gara Formation, Kurdistan Region, Iraq. Iraqi Geological Journal, volume. 53 (1A), pp. 90-116.

Odoma A. N., Obaje N. G., Omado J. I., Idakwo S. O. and Erbacher J. (2015). Mineralogical, chemical composition and distribution of rare earth elements in clay-rich sediments from southeastern Nigeria; Journal African Earth Science, volume.102, pp. 50–60.

Pettijohn, F.J., Potter, P.E. and Siever, R. (1987). Sand and Sandstone. Springer, New York, pp. 553 – 617.

Pittman, E. D. (1988). Diagenesis of Terry sandstone (Upper Cretaceous), Spindle Field, Colorado. Journal of Sedimentary Petrology, volume. 58, pp. 785–800.

Ramos-Vázquez, M., Armstrong-Altrin, J.S., Rosales-Hoz, L., Machain-Castillo, M.L., and Carranza-Edwards, A. (2017). Geochemistry of deep-sea sediments in two cores retrieved at the mouth of the Coatzacoalcos river delta, Western Gulf of Mexico, Mexico. Arabian Journal of Geosciences, volume 10 (6), pp. 148.

Ramseyer, K., Boles, J. R., and Lichtner, P. C. (1992). Mechanisms of Plagioclase Albitization: Journal of Sedimentary Petrology, volume 62, pp. 349–356.

Roser, B.P., Korsch, R.J. (1986). Determination of tectonic setting of sandstone– mudstone suites using SiO2 content and K2O/Na2O ratio. Journal Geology, volume 94, pp. 635–650.

Roser, B.P., Korsch, R.J. (1988). Provenance signatures of sandstone – mudstone suites determined using discriminant function analysis of major-element data. Chemical Geology, volume 67, pp. 119–139.

Seiver, R. (1979). Plate tectonic controls on diagenesis. Journal Geology, volume 87, pp. 127-155.

Sengupta, S.M. (1994). Introduction to sedimentology. Oxford & IBH Publishing Co., pp. 314.

Singh, Y., Haq, A.U., Pandita, S.K., Lone, B.A., Singh, A. (2023). Geoengineering properties of the Sandstones of Upper Murree Formation, Jammu and Kashmir: A case study. Journal Indian Association of Sedimentologists, 40(1), pp. 73-80.

Surdam, R.C. and Boles, J.R. (1979). Diagenesis of volcanic sandstones, In: Scholle, P.A. and Schluger, P.R. (eds.), Aspects of diagenesis: SEPM. Spec. Publ., volume 26, pp. 227-242.

Suttner, L.J., Dutta, P.K. (1986). Alluvial sandstone composition and paleoclimate, framework mineralogy. Journal of Sedimentary Petrology, volume 56, pp. 329-345.

Tawfik, H.A., Salah, M.K., Maejima, W., Armstrong-Altrin, J.S., Abdel-Hameed, A-M.T., Ghandour M.M.E. (2018). Petrography and geochemistry of the Lower Miocene Moghra sandstones, Qattara Depression, north Western Desert, Egypt. Geological Journal, volume 53, pp. 1938-1953.

Taylor, J.M. (1950). Pore-space reduction in sandstones. Bulletin of the American Association Petroleum Geologists 34, pp. 701–716.

Verma S. P. and Armstrong-Altrin J. S. (2013). New multidimensional diagrams for tectonic discrimination of siliciclastic sediments and their application to Precambrian basins. Chemical Geology, 355, pp. 117–180.

Verma, S.P., Armstrong-Altrin, J.S. (2016). Geochemical discrimination of siliciclastic sediments from active and passive margin settings. Sedimentary Geology, volume. 332, pp. 1-12.

Verma, S.P., Díaz-González, L., Armstrong-Altrin, J.S. (2016). Application of a new computer program for tectonic discrimination of Cambrian to Holocene clastic sediments. Earth Science Informatics 9, pp. 151-165.

Winchester, J. A. & Max, M. D. (1989). Tectonic setting discrimination in clastic sequences: an example from the Late Proterozoic Erris Group, NW Ireland. Precambrian Research, volume 45, pp. 19-201.

Zaid S. M. (2016). Geochemistry of shales from the Upper Miocene Samh Formation, north Marsa Alam, Red Sea, Egypt: Implications for source area weathering, provenance, and tectonic setting; Arabian Journal of Geoscience, volume 9, pp. 593.